The Effects of Polar and/or Ionizable Residues in the Core and Flanking Regions of Hydrophobic Helices on Transmembrane Conformation and Oligomerization†

Scott Lew, Jianhua Ren, and Erwin London*

Department of Biochemistry and Cell Biology and Department of Chemistry, State University of New York at Stony Brook, Stony Brook, New York 11794-5215

Received March 28, 2000; Revised Manuscript Received June 6, 2000

ABSTRACT: To explore the influence of amino acid composition on the behavior of membrane-inserted α-helices, we examined the behavior of Lys-flanked polyleucyl (pLeu) helices containing a single polar/ionizable residue within their hydrophobic core. To evaluate the location of the helices within the membrane by fluorescence, each contained a Trp residue at the center of the sequence. When incorporated into dioleoylphosphatidylcholine (DOPC) model membrane vesicles, pLeu helices with or without a single Ser, Asn, Lys, or Asp residue in the hydrophobic core maintained a transmembrane state (named the N state) at neutral and acidic pH. In this state, the central Trp exhibited highly blue-shifted fluorescence, and fluorescence quenching by nitroxide-labeled lipids showed it located at the bilayer center. A state in which Trp fluorescence red-shifted by several nanometers (named the B state) was observed above pH 10−11. B state formation appears to result from deprotonation of the flanking Lys residues. Despite the red shift in Trp emission, fluorescence quenching showed that in the B state the Trp at most is only slightly shallower than in the N state, suggesting the B state also is a transmembrane or near-transmembrane structure. The B state is characterized by increased helix oligomerization, as shown by the dependence of Trp λ_{max} on the concentration of the peptide within the bilayer at high pH. The pLeu peptide with a Asp residue in the core underwent a pH-dependent transition at a lower pH than the other peptides (pH 8−9). At high pH, it exhibited both a more highly red-shifted fluorescence and shallower Trp location than the other peptides. This state (named the S state) did not exhibit a concentration-dependent Trp λ_{max}. We attribute S state behavior to the formation of a charged Asp residue at high pH, and a consequent movement of the Asp toward the membrane surface, resulting in the formation of a nontransmembrane state. We conclude that a polar or ionizable residue can readily be tolerated in a single transmembrane helix, but that the charges on ionizable residues in the core and regions flanking the helix significantly modulate the stability of transmembrane insertion and/or helix−helix association.

Hydrophobic α-helices are the most common structural elements of membrane proteins. High-resolution structures of transmembrane proteins and statistical analysis of sequence data show transmembrane helices frequently contain several polar residues (*1, 2*). In transmembrane proteins with multiple transmembrane helices, the polar residues often face away from lipid, and are believed to stabilize interhelical interactions. However, such interhelical interactions can be driven by van der Waals interactions between nonpolar side chains instead of polar interactions (*3, 4*). Furthermore, polar residues are also found in membrane proteins with a single transmembrane helix (*2*). Whether such residues contact lipid or instead are involved in noncovalent interactions with helices on other membrane proteins is generally unknown. Thus, the exact roles that polar residues play in maintaining the structure of transmembrane segments of membrane proteins is unclear.

There is also little information on the effects of ionizable residues introduced into single hydrophobic helices. In some cases, it appears they can strongly influence structure and helix−helix oligomerization (*5, 6*). We have previously shown that a single Asp residue can even be accommodated in a single transmembrane helix (*7*). A recent study of von Heijne and co-workers shows that ionizable residues can also be placed in the core of the tramsmembrane segment in a simple model of two and three helix proteins (*8*). On the other hand, ionizable residues are rare in transmembrane sequences of proteins with single transmembrane spanning segments (*2*).

In this study, polar and ionizable residues were introduced into derivatives of poly Leu polypeptides in order to examine their effects on the behavior of hydrophobic helices inserted into membranes. Lys-flanked poly Leu (pLeu) polypeptides are a useful system for such studies as they form simple hydrophobic helices which have a fully transmembranous conformation when the length of the helix-forming poly Leu stretch matches the width of the bilayer (*9*−*12*). The location of such hydrophobic helices within the lipid bilayer can be assessed by inclusion of a Trp residue within the core of the sequence (*7, 9, 11, 12*). We find that the presence of polar and ionizable residues can be tolerated in the transmembrane state. However, the protonation states of ionizable residues both in the core of the hydrophobic helix and in the

† This work was supported by NIH Grant GM 48596.

* Correspondence should be addressed to this author. Phone: (631) 632-8564. Fax: (631) 632-8575. Email: Erwin.London@sunysb.edu.

10.1021/bi000694o CCC: $19.00
Published on Web 07/20/2000

sequences flanking the hydrophobic region have significant effects on helix behavior.

EXPERIMENTAL PROCEDURES

Materials. The pLeu[1] peptides $K_2GL_9WL_9K_2A$ [pLeu(L11)], $K_2GL_7DLWL_9K_2A$ [pLeu(D11)], $K_2GL_7KLWL_9K_2A$ [pLeu(K11)], $K_2GL_7SLWL_9K_2A$ [pLeu(S11)], $K_2GL_7NLWL_9K_2A$ [pLeu(N11)], and $R_2GL_9WL_9R_2A$ [pLeu(R1,2,23,24,L11)] were purchased from Research Genetics, Inc. (Huntsville, AL). All the peptides had acetylated N-termini and amide-blocked C-termini. The phosphatidylcholines (PCs, 1,2-diacyl-*sn*-glycero-3-phosphocholines) di 18:1Δ9c PC (dioleoyl-PC, DOPC), di 22:1Δ13c PC (dierucoyl-PC, DEuPC), 5 or 12 SLPC [1-palmitoyl-2-(5- or 12-doxyl)stearoyl-PC], and TempoPC [1,2-dioleoyl-*sn*-glycero-3-[4-(*N*,*N*-dimethyl-*N*-(2-hydroxyethyl)ammonium]-2,2,6,6-tetramethylpiperidine-1-oxyl] were purchased from Avanti Polar Lipids, Inc. (Alabaster, AL).

Peptides were purified with a reversed-phase C18 column (*14*). Mobile phase mixtures of 0.5% trifluoroacetic acid/2-propanol (v/v) and 0.5% trifluoroacetic acid/H_2O were used to elute peptides using 2-propanol gradients at a flow rate of 0.4 mL/min. Elution of the purified peptides generally occurred between 50% and 70% 2-propanol. The desired fractions were then dried and redissolved in ethanol. It should be noted that in a previous study (*12*), in which it was necessary to label peptides in some experiments, the pH value of the peptide solution was adjusted to near neutral with NaOH prior to storage at −20 °C. For our study, pH neutralization was omitted. The purity of the peptides was confirmed with MALDI-TOF mass spectrometry (Center for the Analysis and Sequence of Macromolecules, SUNY, Stony Brook) using α-cyanohydroxycinnamic acid as the matrix and bovine insulin as a molecular weight standard. Any impurities remaining were minor, and generally peptides with a one or two amino acid deletion. Peptide concentration was determined from the UV absorbance at 280 nm by using $\epsilon = 5500\ M^{-1}\ cm^{-1}$.

Spectroscopic Measurements. Absorbance was measured in 1 cm quartz cuvettes on a Beckman 650 spectrophotometer. Tryptophan fluorescence (excitation wavelength 280 nm) was measured on a SPEX τ2 fluorolog spectrofluorometer operating in the steady-state mode. Unless otherwise noted, f luorescence and fluorescence quenching measurements to determine Trp depth were made in a semimicro quartz cuvette (1 cm excitation path length and 4 mm emission path length) using a 2.5 mm excitation slit and 5 mm emission slit. However, in samples in which the pH was titrated, fluorescence measurements were made in a 1 cm path length cuvette. For these experiments, slits of 5 mm were used for both excitation and emission. Circular dichroism (CD) spectra were recorded as previously described using a JASCO J-715 CD spectrometer with a 1 mm quartz cuvette at room temperature (*7, 12*).

[1] Abbreviations: DOPC, dioleoyl-*sn*-glycero-3-phosphocholine; DEuPC, dierucoyl-*sn*-glycero-3-phosphocholine; pLeu(L11), $K_2GL_9WL_9K_2A$; pLeu(D11), $K_2GL_7DLWL_9K_2A$; pLeu(K11), $K_2GL_7KLWL_9K_2A$; pLeu(S11), $K_2GL_7SLWL_9K_2A$; pLeu(N11), $K_2GL_7NLWL_9K_2A$; pLeu(R1,2,23,24,L11), $R_2GL_9WL_9R_2A$; 5 or 12 SLPC, 1-palmitoyl-2-(5- or 12-doxyl)stearoyl-PC; TempoPC, 1,2-dioleoyl-*sn*-glycero-3-[4-(*N*,*N*-dimethyl-*N*-(2-hydroxyethyl)ammonium]-2,2,6,6-tetramethylpiperidine-1-oxyl.

Procedure for pH Titration Experiments. To measure peptide fluorescence as a function of pH, vesicles were made by dilution from ethanol as previously described (*7, 12*). The appropriate aliquots of the desired lipids and peptides dissolved in ethanol were mixed, dried under nitrogen, and then redissolved in 40 μL of ethanol. The samples were then diluted with 1960 μL of pH 7.6, 10 mM sodium phosphate, 150 mM NaCl. Final peptide concentration was 2 μM, and lipid concentration was 200 μM. Duplicate samples were prepared. Background samples were prepared using the same protocol except peptide was omitted. After the dilution with phosphate buffer as described above, a small aliquot of concentrated acetic acid (4−5 μL) was used to lower the pH to the desired value. For each sample, an emission spectrum was scanned from 300 to 360 nm. For increasing pH by titration, successive aliquots of 0.5−2 M NaOH were used. After each addition of NaOH, the emission spectrum was remeasured. At the end of the titration, the pH was 11.5−12 and about 140 μL of NaOH had been added. Samples lacking peptide were used as background, and subtracted to yield the final spectra.

Procedure for Measurements on Individual Samples Having Different pH. To prepare individual samples at different pH values, vesicles with DOPC and peptide were made by ethanol dilution as described above, except that all volumes were decreased by a factor of 2 and each sample was made with a different buffer. The following buffers were used: 61 mM citric acid, 77 mM Na_2HPO_4, pH 4; 37 mM citric acid, 126 mM Na_2HPO_4, pH 6; 10 mM sodium phosphate, pH 7.6; 50 mM glycine, 8.8 mM NaOH, pH 9; 50 mM glycine, 32 mM NaOH, pH 10; 25 mM Na_2HPO_4, 4.1 mM NaOH, pH 11; and 25 mM Na_2HPO_4, 23 mM NaOH, pH 11.9. All buffers had 150 mM NaCl. The final lipid concentration was 200 μM, and the final peptide concentration was 2 μM. The final volume for all samples was 1 mL. As usual, background samples without peptide were also prepared.

Procedure for Measurement of Trp Depth. To measure Trp depth, vesicles were made by dilution from ethanol essentially as described for the titration experiments, except that samples contained either DOPC or a mixture of DOPC and enough of the quencher-labeled lipid (either TempoPC, 5 SLPC, or 12 SLPC) to give 15 mol % of active nitroxide (*15*), and the volumes were all decreased by a factor of 2. The appropriate aliquots of the desired lipids dissolved in ethanol were mixed, dried under nitrogen, and then dissolved in 20 μL of ethanol. The samples were then diluted with 980 μL of pH 4, 7.6, or 11.5−12 buffer (10 mM sodium phosphate, 150 mM NaCl titrated to pH 4 with concentrated acetic acid or pH 11.5−12 with NaOH if desired). The final peptide concentration was 2 μM, and the lipid concentration was 200 μM. Duplicate samples were prepared. Background samples were prepared using the same protocol except peptide was omitted. Emission intensity was measured at room temperature at the wavelength of maximum intensity in the sample lacking quencher (i.e. 100% DOPC). The fluorescence intensity of background samples was subtracted, and then the ratio of fluorescence in the vesicles containing quencher lipid (F) to that in the vesicles in which the only lipid was DOPC (F_o) was calculated. The distance of the Trp from the center of the bilayer (z_{cf}) was calculated as

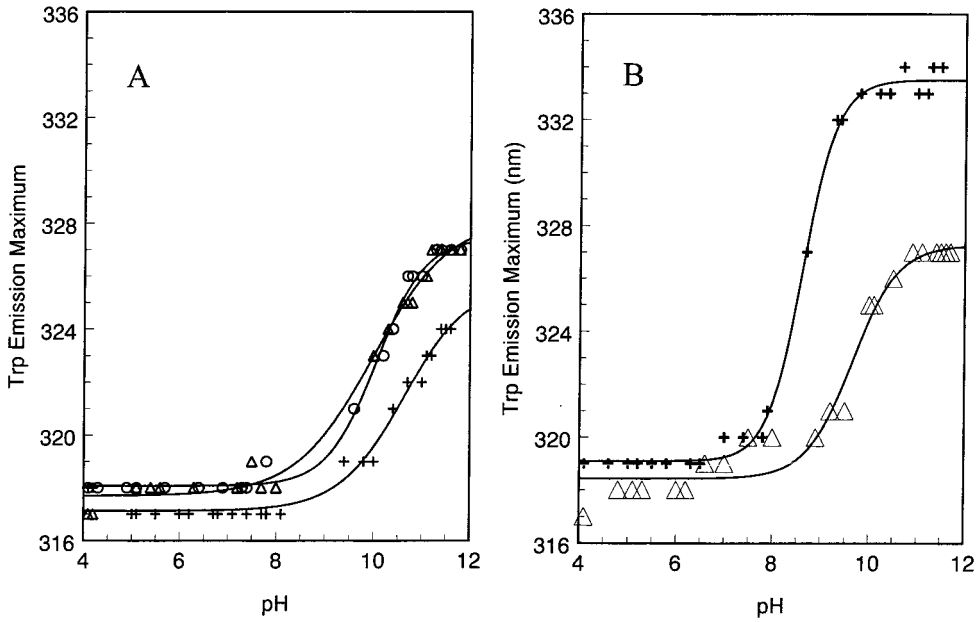

FIGURE 1: Effect of pH on the wavelength of maximum Trp emission for pLeu peptides incorporated in DOPC vesicles as determined by titrating pH. Peptide concentration was 2 μM, and lipid concentration was 200 μM. Samples were prepared at low pH, and then each was titrated to high pH with aliquots of NaOH, measuring the fluorescence after each aliquot. The data shown are the average for two sets of samples fit to a sigmoidal curve. Sample λ_{max} generally differed from the average by $\pm 1-2$ nm. (A) (+) pLeu(L11), (○) pLeu(S11), (△) pLeu(N11); (B) (+) pLeu(D11), (△) pLeu(K11).

described previously, using the equation appropriate for Trp residues close to the bilayer center (*7*).

Procedure for Measuring λ_{max} vs Concentration. Samples with peptide and DOPC were made by ethanol dilution as described above. The peptide concentration was 2 μM. Lipid concentration was either 200 or 1000 μM. After the dried lipid/peptide mixtures were dissolved in 20 μL of ethanol, they were then diluted to 1 mL with either 10 mM sodium phosphate, 150 mM NaCl, pH 7.6, or 10 mM sodium phosphate, 150 mM NaCl, pH 11.7. Duplicate samples were prepared, and the values reported were determined after subtraction of intensity in background samples lacking peptide.

Procedure for Measuring Circular Dichroism. For circular dichroism measurements, 1 mL samples were prepared by ethanol dilution as described above in the following buffers (1:10 dilutions of buffers mentioned above with water): 6.1 mM citric acid, 7.7 mM Na_2HPO_4, 15 mM NaCl, pH 4; 1 mM sodium phosphate, 15 mM NaCl, pH 7.6; and 2.5 mM Na_2HPO_4, 2.3 mM NaOH, 15 mM NaCl, pH 11.3. Peptide concentration was 2.5 μM, and lipid concentration was 200 μM.

RESULTS

Analysis of Transmembrane Insertion in DOPC Model Membrane Vesicles. The behavior of a series of model membrane-bound, Lys-flanked, polyleucyl (pLeu) peptides was compared. The peptides studied (general sequence K_2-$GL_7XLWL_9K_2A$) had a guest residue, Leu, Ser, Asn, Lys, or Asp, in the core of the hydrophobic sequence at position X (residue 11) and are named pLeu(L11), pLeu(S11), pLeu-(N11), pLeu(K11), and pLeu(D11), respectively.

First, the λ_{max} of fluorescence for the various bilayer-incorporated pLeu peptides as a function of pH was examined. Previous studies have shown that for a Trp in the center of the hydrophobic sequence of a pLeu peptide a λ_{max} in the 316−319 nm range is indicative of a transmembrane helix with the Trp located at the center of the bilayer. There is a progressive red shift in the Trp fluorescence emission λ_{max} as the Trp group is moved toward the membrane surface (*7*, *12*). Figure 1 shows that in the pH range 4−8 all of the pLeu peptides studied exhibited λ_{max} in the range 317−319 nm when incorporated in DOPC vesicles. This indicates that these peptides all form a transmembrane structure around neutral pH. However, upon titration to very high pH, the peptides underwent a change which resulted in a red shift of Trp emission (Figure 1). We named the conformation predominating at low pH the N state (for neutral pH state), and that at high pH the B state (for basic pH state). The value of λ_{max} in the B state appears to be in the range 324−328 nm for the pLeu(N11), pLeu(L11), pLeu(K11), and pLeu(S11) peptides.[2] For these peptides, the change from the N to the B state appears to begin at pH 9, perhaps being half-complete at about pH 10−11 in most cases. The behavior of pLeu(D11) was different than that of the other peptides (Figure 1B). It converted into a high-pH state above pH 8, with a midpoint of about pH 8.5−9, and at high pH it exhibited significantly more red-shifted fluorescence at

[2] In addition to a red shift of fluorescence, a shoulder arising from an even more red-shifted species was observed at high pH. This species was most abundant in the pLeu(N11), in which case we could estimate its λ_{max} of emission was close to that of Trp in water (360 nm on our instrument). This species does not arise from peptide that has dissolved in water, as its fluorescence was as strongly quenched by nitroxide-labeled lipid as the main Trp peak. It does not appear to be the product of an irreversible chemical reaction, as its formation was found to be reversible when the pH in a sample was returned to near-neutral. The amount of the species was also dependent on peptide concentration, being more abundant at high concentration (data not shown). We speculate that this highly red-shifted species represents some oligomeric state in which the Trp is hydrogen bonded to some polar species, such as a trapped water molecules, or a polar residue. Some nonpeptide impurity may also be involved as the amount of the highly red-shifted species seemed to vary in amount in different preparations of peptide.

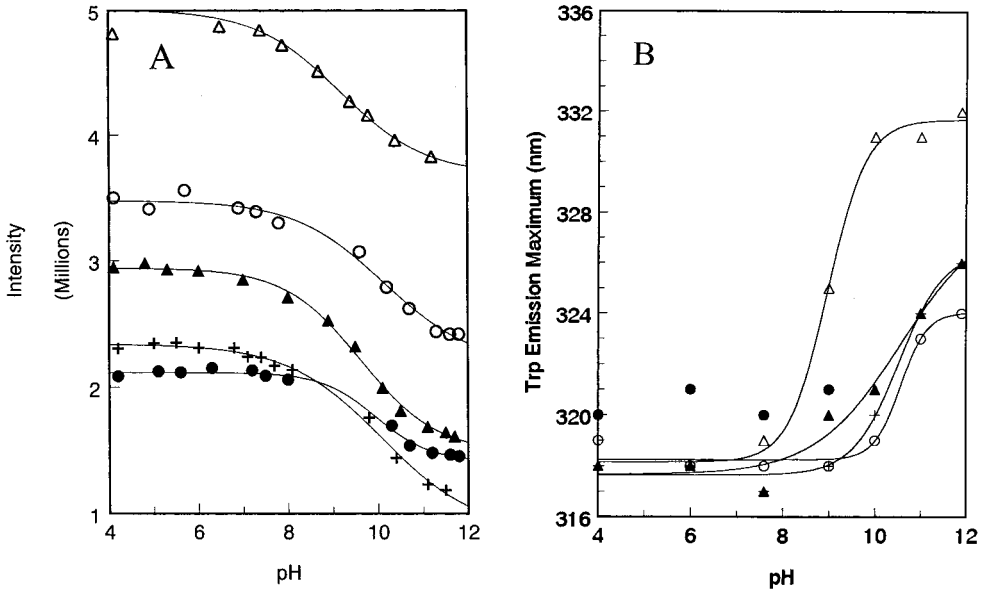

FIGURE 2: Effect of pH on Trp emission. (A) Effect of pH on fluorescence intensity at 330 nm. Sample prepared as above. Intensities shown are after correction for dilution. (+) pLeu(L11), (○) pLeu(S11), (●) pLeu(N11), (△) pLeu(D11), (▲) pLeu(K11). (B) Effect of pH on the wavelength of maximum Trp emission for pLeu peptides incorporated in DOPC vesicles on samples prepared at different pH values. Peptide concentration was 2 μM, and lipid concentration was 200 μM. Samples were prepared at the final desired pH. Other conditions as in Figure 1. (+) pLeu(L11), (○) pLeu(S11), (●) pLeu(N11), (△) pLeu(D11), (▲) pLeu(K11).

high pH than the other peptides (333 nm). We named this high-pH state the S state.

These transitions can also be detected by the change in fluorescence intensity because the species present at high pH fluoresce more weakly than the N state at 330 nm (Figure 2A). The transitions occur at about the same pH as that detected by λ_{max}. (In principle, intensity changes are more linear in the concentration of the species involved than λ_{max}, which is weighted toward the most fluorescent species present. However, intensity changes can be a little more variable than λ_{max} in some cases, and we tended to rely on the latter.) Because of the decrease in intensity at high pH, either there was no isoemissive wavelength, or it was difficult to detect. There are no conclusions we can draw about the number of species that exist at low and high pH in this case.

Results similar to those obtained in the titration experiments were also obtained when individual samples of each peptide were prepared at different pH values (Figure 2B). This indicates that the rate of equilibration of pH across the bilayer is not a factor affecting the pH at which the N to B change occurs. In addition, when samples were prepared at high pH and then the pH was reversed to neutral, the red shift was reversed (data not shown). This indicates that the structural change at high pH is reversible, and rules out artifacts from irreversible reactions such as high pH-catalyzed lipid degradation.

Together, the experiments above indicate that the change in peptide structure is due to some ionization event at high pH. The only ionizable residues common to all of the peptides are the Lys residues that flank the hydrophobic sequence, two on each side. Therefore, the change at high pH must involve Lys deprotonation. This conclusion is supported by the fact that the pK_a of Lys in solution occurs at about the same range (pH 10−11) as the change from the N to B states. That the ionization values are similar for Lys residues in solution and flanking a hydrophobic helix are similar is not surprising as the Lys residues flanking the hydrophobic sequence probably protrude into the aqueous environment beyond the ends of the hydrophobic core of the bilayer (*35*).

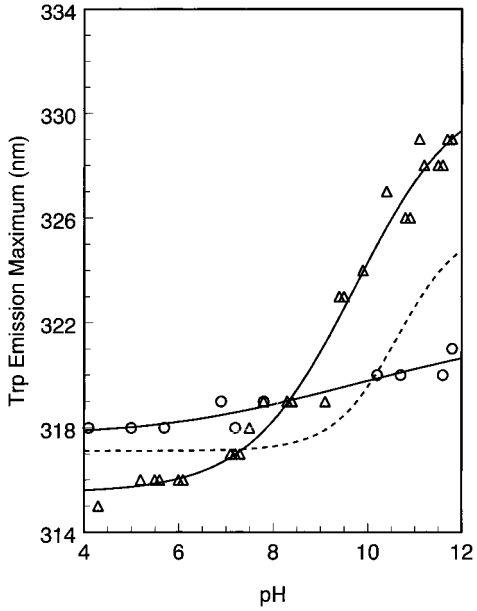

FIGURE 3: Effect of pH on the wavelength of maximum Trp emission for (○) Arg-flanked pLeu peptide [pLeu(R1,R2,R23,R24,-L11)] incorporated in DOPC vesicles, and (△) pLeu(L11) incorporated into DEuPC bilayers. The dashed line shows the behavior of pLeu(L11) in DOPC from the data in Figure 1. Conditions as in Figure 1.

To help confirm the role of flanking residue deprotonation, the pH dependence of the λ_{max} of fluorescence of a peptide in which the flanking Lys residues are replaced by Arg (R_2-$GL_9WL_9R_2A$) was measured. Only a very weak pH dependence of fluorescence was observed up to pH 12 (Figure 3) as would be predicted if deprotonation of the flanking residues is the cause of the red shift at high pH (because the pK_a of Arg is several units higher than that of Lys). At this

Table 1: Distance of the Central Trp Residue from the Bilayer Center (z_{cf}) As Determined from the Level of Fluorescence Quenching by Nitroxide-Labeled Lipids

		F/F_o[a]			
peptide	pH	shallow quencher	medium depth quencher	deep quencher	z_{cf} (Å)
pLeu(L11)	4	0.70 ± 0.06	0.55 ± 0.02	0.09 ± 0.02	1.0
	7.4	0.67 ± 0.02	0.59 ± 0.02	0.09 ± 0.01	0.5
	11.7	0.92 ± 0.03	0.81 ± 0.04	0.22 ± 0.01	1.3
pLeu(S11)	4	0.73 ± 0.03	0.56 ± 0.06	0.08 ± 0.01	0.5
	11.7	0.82 ± 0.03	0.70 ± 0.06	0.16 ± 0.02	1.2
pLeu(N11)	4.1	0.62 ± 0.06	0.47 ± 0.09	0.09 ± 0.04	1.9
	11.7	0.85 ± 0.08	0.68 ± 0.03	0.22 ± 0.03	2.4
pLeu(D11)	4	0.75 ± 0.03	0.52 ± 0.02	0.10 ± 0.04	1.6
	11.9	0.65 ± 0.06	0.54 ± 0.06	0.23 ± 0.02	3.9
pLeu(K11)	4	0.76 ± 0.07	0.52 ± 0.02	0.10 ± 0.02	1.6
	12	0.89 ± 0.07	0.74 ± 0.04	0.26 ± 0.03	2.3

[a] F/F_o is the ratio of the Trp fluorescence intensity of pLeu peptides incorporated into vesicles containing DOPC and 15 mol % nitroxide-labeled lipid to the fluorescence intensity of pLeu peptides incorporated in DOPC vesicles; i.e., it is the fraction of unquenched fluorescence. z_{cf} is the distance of the central Trp residue from the bilayer center, calculated from quenching as described in (*7*). The shallow quencher was TempoPC, medium depth quencher 5 SLPC, and deep quencher 12 SLPC. Samples contained 2 μM peptide and 200 μM total lipid. Four experiments were performed for each set of conditions. Standard deviations are shown.

time, we cannot determine which of the flanking Lys deprotonate when the red shift occurs. However, it is unlikely that different flanking Lys have very different pK_a values.

The difference between the effect of pH on pLeu(D11) and that of the other Lys-flanked peptides indicates that pLeu(D11) has very different ionization properties. As described below, this difference probably reflects ionization of the Asp residue of pLeu(D11) at high pH.

Analysis of Insertion Depth by Parallax Analysis of Fluorescence Quenching. One possibility for the origin of the red shift of Trp fluorescence at high pH is that it could result from their movement to a more polar environment. This could happen if the peptides were moving toward the membrane surface at high pH. However, a red shift in fluorescence emission wavelengths is sensitive to more than just Trp depth in the bilayer. λ_{max} is subject to polarization artifacts and can be affected by local interactions and solvent relaxation effects (*16*). Furthermore, it can respond to oligomerization [(*12*) and see below].

Therefore, to see if Trp depth was affected by high pH, fluorescence quenching by nitroxide-labeled phospholipids was used to measure Trp depth. In this method, the depth of a fluorophore is calculated from the ratio of its quenching by lipids carrying a nitroxide (spin) label at different depths (*15, 17*). We have previously shown that this method (parallax analysis) can give accurate depths in a wide variety of cases (*15, 17*−*22*), including transmembrane peptides (*7*).

Table 1 shows the amount of quenching induced by nitroxide-labeled lipids, and estimated distances of the Trp residue from the bilayer center (z_{cf}) for the pLeu peptides incorporated into DOPC-containing bilayers. For all of the peptides, the Trp, which is at the center of the hydrophobic sequence, locates close to the bilayer center in the N state (z_{cf} average 1.3 ± 0.7 Å), as expected for a transmembrane structure (*5*). At high pH, there was in almost all cases at most only a small movement toward a shallower depth [z_{cf} average 1.8 ± 0.6 Å, not counting pLeu(D11); see below]. This suggests that even in the B state most of the peptides remain deeply buried in the bilayer, and in fact are likely to remain in a transmembrane state (see Discussion). [A Trp depth within 1 Å from the bilayer center was also measured, both at low pH and at pH 11.9, for the peptide with flanking Arg residues (data not shown).]

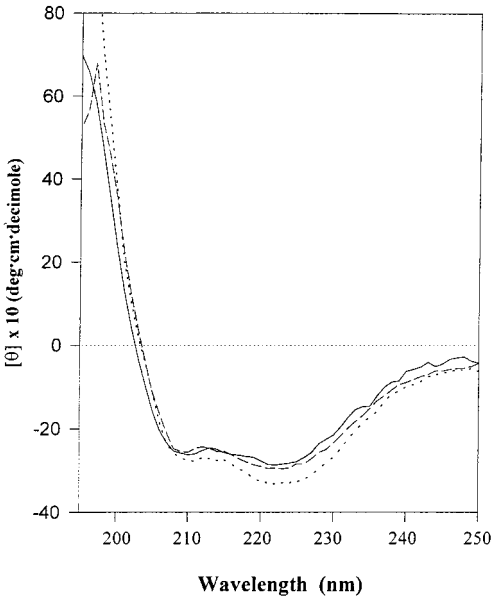

FIGURE 4: CD spectra of pLeu(L11) in DOPC vesicles. Peptide concentration was 2.5 μM and lipid concentration 200 μM. Spectra were measured at (− −) pH 4, (—) pH 7, and (· · ·) pH 11.

The one exception to this behavior at high pH was pLeu(D11), in which the Trp shifts to 3.9 Å from the bilayer center at high pH. Qualitiatively, the decrease in depth of pLeu(D11) at high pH is illustrated by the fact that quenching by the shallow quencher TempoPC increases at high pH, whereas that by the deep quencher 12 SLPC decreases. This pattern is not observed for any of the other peptides. Also, as noted above, pLeu(D11) shows the most red-shifted fluorescence at high pH. Therefore, it appears that the membrane-inserted D11 peptide takes on a shallower location at high pH. We named this form the S state (for shallow or surface state). The simplest explanation for the behavior of pLeu(D11) at high pH is that it is due to the deprotonation of its Asp to form a charged state. An inability to bury a charged Asp residue in the membrane would result in the movement of the pLeu(D11) helix toward the membrane surface, resulting in a shallower Trp depth and large red shift in λ_{max} (see Discussion).

Secondary Structure of pLeu Peptides. The experiments above show that for the pLeu peptides [other than pLeu(D11)] the change at high pH does not involve a major change in Trp depth. However, it is possible that the change at high pH could involve a large change in secondary structure. To examine the secondary structure, and its pH dependence, circular dichroism (CD) spectra of the peptides incorporated into DOPC vesicles were measured. Figure 4 shows CD spectra for pLeu(L11). The spectral shapes and intensities found are characteristic of highly helical peptides (*7*). There may be a slight increase in α-helix at high pH as shown the stronger negative intensity in the 200−220 nm region. Similar spectra at both high and low pH were

Table 2: Effect of pLeu Peptide Concentration within the Lipid Bilayer on λ_{max} of Trp Fluorescence Emission[a]

peptide	pH	lipid concn (μM)	λ_{max} (nm)
pLeu(L11)	7.6	200	318
		1000	318
	11.7	200	324
		1000	321
pLeu(S11)	7.6	200	318
		1000	318
	11.7	200	325
		1000	321
pLeu(N11)	7.6	200	319[b]
		1000	319
	11.7	200	328
		1000	324
pLeu(D11)	7.6	200	319
		1000	318
	11.7	200	330
		1000	331
pLeu(K11)	7.6	200	318
		1000	318
	11.7	200	325
		1000	322

[a] Samples contained 2 μM peptide. The values shown are the average of duplicate experiments. They were reproducible to $\pm 1-2$ nm. [b] pLeu(N11) value at pH 7.6 is for peptide in citrate buffer. A value of 324 nm was found in 10 mM sodium phosphate, 150 mM NaCl, pH 7.6. This red shift appears to be due to a metal ion contaminant removed by chelation with citrate. A value of 319 nm was also obtained in 10 mM sodium phosphate, 150 mM NaCl, pH 7.6, containing EDTA. (Red shifts seen at pH 11.7 were not abolished by the addition of citrate.) We do not know if this contaminant is specific to pLeu(N11) or simply affects this peptide more than the others studied.

obtained for all of the other peptides, indicating they have about the same helix content as pLeu(L11) (data not shown).

Dependence of Emission λ_{max} upon Peptide Concentration within the Bilayer. For peptides other than pLeu(D11), the experiments above suggest that in most cases neither a change in Trp depth nor a change in secondary structure can explain why Trp fluorescence red-shifts at high pH. An alternate explanation for this red shift is that it is due to helix oligomerization. We found previously that pLeu peptides with a Trp in center of the hydrophobic sequence exhibit a red-shifted λ_{max} when they form oligomers, and a blue-shifted λ_{max} when in a monomeric or very small oligomeric state (*12*).

To test for oligomerization, Trp fluorescence λ_{max} was compared at a high and low peptide concentration within the bilayer. This was done by incorporating the peptide in vesicles with either a 200 or 1000 μM DOPC concentration, respectively. As shown in Table 2, the red shift of fluorescence at high pH was significantly reduced when the concentration of the helices in the bilayer was diluted (i.e., the red shift was less in 1000 μM DOPC relative to that in 200 μM DOPC). The decrease in red shift indicates a decrease in oligomeric size upon dilution (*12*). The one exception to this behavior was pLeu(D11), for which the fluorescence remained highly red-shifted at both concentrations at high pH. A lack of a concentration dependence of the fluorescence λ_{max} was also observed for all the peptides at pH 7.6, where pLeu peptides appear to be in a monomeric or low-oligomeric state (*12*). These results indicate that pLeu helices show a stronger tendency to oligomerize at high pH relative to neutral pH. Another hint that there is more oligomerization at high pH comes from queching data. At high pH, there tends to be less quenching by **all** of the quenchers. This type of change is expected for oligomerization, which would tend to prevent Trp contact with lipid, although a decrease in the excited-state lifetime for Trp at high pH could also contribute to the decreased quenching.

One possible explanation for increased oligomerization at high pH is that the electrostatic repulsions between flanking Lys residues on different helices, which would inhibit oligomerization, are lost upon Lys deprotonation. Other contributions to increased oligomerization at high pH are considered under Discussion.

Effect of Mismatch between Bilayer Width and Peptide Length on the Sensitivity of pLeu Peptides to pH. In previous studies, we found that when there is hydrophobic mismatch such that the width of the hydrophobic core of the bilayer exceeds hydrophobic helix length pLeu peptides remain helical, but their transmembrane orientation is significantly destabilized relative to a location close to the bilayer surface (*7*). To see if the N to B conformational change would be sensitive to bilayer width, the pH dependence of pLeu(L11) behavior was examined in vesicles prepared from dierucoylphosphatidylcholine (DEuPC). In contrast to DOPC, which has 18 carbon acyl chains, DEuPC has 22 carbon acyl chains, and forms bilayers about 7 Å wider than those of DOPC. Both lipids have one double bond near the center of the acyl chains and form fluid state bilayers at room temperature (*23*).

Figure 3 shows the fluorescence emission of pLeu(L11) in DEuPC bilayers as a function of pH. As in DOPC bilayers, fluorescence is blue-shifted at low pH and red-shifts at high pH (Figure 3). The red shift at high pH is reduced by peptide dilution in the bilayer (not shown). However, in DEuPC the apparent pK_a of the N to B state transition appears to be lower (by up to 1 pH unit), and the amount of the red shift greater, than they are in DOPC. The pK_a change in DEuPC is consistent with the fact that high pH is promoting deprotonation of flanking Lys residues. In DEuPC vesicles, bilayer width is greater than the length of the hydrophobic sequence (*7*). This mismatch should result in the flanking Lys becoming more buried in the hydrophobic regions of the bilayer relative to their degree of burial in DOPC. In this more hydrophobic environment, they should form the uncharged deprotonated state more readily than in DOPC. Another contribution to the change in flanking Lys pK_a may come from the fact that oligomerization, which appears to be more extensive in the B state, can decrease the energetic cost of unfavorable mismatch between bilayer width and length (see Discussion).

DISCUSSION

Properties of pLeu Helices in the N and B States. Figure 5 summarizes a model for the location of hydrophobic pLeu helices within the bilayer in the N and B states. Previous studies have shown the N state, which predominates at neutral pH, to be in the form of a transmembrane helix (*7*, *12*). The high-pH-induced B state results from the loss of charge on helix-flanking residues. It is a helical structure based on circular dichroism. It is also likely to be a transmembrane or near-transmembrane (if the ends of the peptide do not quite reach the surface) structure based on

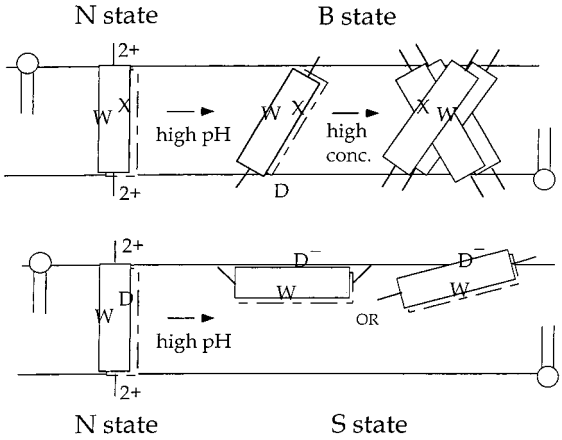

FIGURE 5: Schematic figure showing the proposed helix properties in the N, B, and S states. Note that the exact ionization state of the flanking Lys at high pH may depend on pH, and that we cannot distinguish between cases in which the flanking Lys residues deprotonate on just one or both sides of the helix. For the Asp peptide, either the N terminal or the C terminal may be membrane-inserted at high pH. Two less likely transmembrane models for the Asp peptide in the S state are described in the text.

the observation that, like the N state, the Trp in the center of the hydrophobic sequence locates very close to the bilayer center. The highly blue-shifted fluorescence seen at high pH when the peptide concentration is diluted also indicates a Trp location within a couple of angstroms from the bilayer center. In addition, even in the uncharged state the terminal amines of the flanking Lys should be relatively polar, and might be expected to locate close to the bilayer surface, as do other polar groups (*19*).

Thus, a nontransmembrane model for the B state in which the ends were deeply buried in hydrophobic region of the bilayer, such that anchoring at the membrane surface is lost, would be surprising. Furthermore, this model would have the helix floating randomly within the core of the bilayer, and would predict a Trp depth closer to the average value for a group randomly distributed at all depths within the hydrophobic core, perhaps 5−7 Å from the bilayer center rather than 1−2 Å. This shallower location would also predict a significant red shift of Trp fluorescence that would not be abolished by dilution of peptide within the bilayer. These behaviors are not detected, arguing against such a model.

Charge on Helix-Flanking Residues Modulates Helix Oligomerization. The most important difference between the N and B state appears to be the tendency of the B state to oligomerize more strongly or to a greater degree than the N state. In fact, the B state shows very similar λ_{max} and depth behavior to another condition previously shown to promote oligomerization at neutral pH, namely, that of peptides longer than necessary to span the bilayer. In that case, it appears that increased helix tilting, needed to prevent exposure of hydrophobic groups to solution, permits strong van der Waals interactions between helices, and thus promotes oligomerization (*12*).

There are several possibilities for how the high-pH-induced deprotonation of the flanking Lys could also favor oligomerization. The most obvious is that electrostatic repulsions between Lys on different helices would be abolished by deprotonation. This factor has recently been proposed to explain the different levels of oligomerization of artificial transmembrane helices in natural membranes (*25*). A second consequence of the loss of charge on flanking Lys resides is that the ends of the helix would become more hydrophobic, resulting in a helix with an effectively longer hydrophobic length. This might allow the helices to bury their ends slightly more deeply in the bilayer. The slight increase in helical content at high pH is consistent with such a change. This increase in effective hydrophobic length would thus allow helix tilting and thereby promote oligomer formation.

Helix behavior in DEuPC vesicles is consistent with a role of electrostatic repulsions in regulating oligomerization. There is easier deprotonation of the Lys residues in DEuPC relative to DOPC, and at the same time an increased red shift, strongly suggestive of a higher level of oligomerization. This is consistent with oligomerization being promoted by the loss of electrostatic repulsions. On the other hand, there are other effects due to the mismatch between helix length and bilayer width. For example, it would be expected in DEuPC that helix tilting is reduced because the helix must span a longer hydrophobic length. This should reduce oligomerization. However, if helix length is too short to easily span the bilayer, previous studies have suggested that oligomerization would be promoted by its tendency to minimize the amount of the high-energy lipid/helix surface boundary, along which there is mismatch strain (Figure 5) (*25*). Although we cannot evaluate the contribution of this factor, we note that the mismatch strain cannot by itself explain oligomerization at high pH, because the expected increase in hydrophobic length resulting from flanking Lys deprotonation at high pH would be expected to reduce such strain.

Single Polar/Ionizable Residues Can Be Accommodated in the Transmembrane State. The pLeu helices studied maintained the N orientation at neutral pH when a polar residue was introduced into the hydrophobic core. This indicates a single polar residue destabilizes the N state too weakly to detect a significant change in the fraction of N state molecules for the strongly hydrophobic polyleucyl sequence. Presumably in a less hydrophobic background, or if the number of polar residues was increased, the effects of such polar residues would be much more pronounced. This is supported by studies indicating the formation of a transmembrane structure is decreased when three polar residues are inserted in the less nonpolar poly Ala helix (*13*). It would be interesting to examine the effect of multiple polar substitutions in a polyLeu sequence, or of a single polar residue in a peptide with an intermediate hydrophobicity, such as an Ala/Leu mixture (*26*, *27*).

Behavior of Helices with Ionizable Residues within the Hydrophobic Core. One of the most striking observations in this report is that a single hydrophobic pLeu helix with a "charged" residue (i.e., Lys or Asp) in its hydrophobic core can maintain a transmembrane state and thus bury such residues deeply within the bilayer. The most likely explanation for this behavior is that ionizable residues in the hydrophobic core of the bilayer exist in their uncharged state. This means their pK_a values have significantly shifted from the values which they have in aqueous solution.

In the case of the Asp peptide, the midpoint of the N to S transition (pH 8.5−9 in DOPC) undoubtedly represents the pK_a of the Asp carboxyl group.[3] This value, 4−5 pH units higher than in aqueous solution, is very unusual, but not really surprising for a membrane-inserted Asp,[4] in view of

the fact that several studies have shown that even when at the membrane surface a carboxyl group has a pK_a shifted up to 7 (*28*).

Figure 5 shows a model for the structure of the Asp-containing pLeu(D11) in the S state. This model for the S state is consistent with studies indicating charged groups reside at least 16 Å from the bilayer center (*21, 29*). In addition, since the Trp is on the side of the helix more or less opposite that of the Asp, it should be facing the interior of the bilayer, and given helix and side chain dimensions should be about 10 Å more deeply located than the Asp (calculation not shown). This predicts a Trp depth close to that determined by fluorescence quenching.[5] [The depth of the Trp would be shallower as judged by the standard curve of Trp depth vs λ_{max} we previously derived. However, that curve does not include effects of oligomerization (*7*).]

It should be noted that since a helical structure is maintained, and since the core pLeu sequence is so hydrophobic, most of the sequence is likely to remain significantly buried within the bilayer in the S state. As a result, one or both of the helix ends may also become buried (Figure 5), and it is likely that deprotonation of the Asp residue at high pH is accompanied by deprotonation of at least some of the flanking Lys residues.

It should be noted that there are two other models for the conformation of pLeu(D11) at high pH which we cannot fully eliminate but seem quite unlikely. One is a model in which pLeu(D11) is transmembranous and the red shift in Trp emission is due to interhelical Trp−Asp interactions (*16*). This model is unlikely because it would predict Trp depth remains at the bilayer center. The second is one in which the Asp group alters the lipid conformation such that one or more lipids have their polar headgroups buried well within the lipid bilayer, and in contact with the Asp group. In this case, the Trp would seem shallower (it would be close to the polar headgroups of some lipid molecules) and red-shifted. It seems unlikely that such a change could occur, but this possibility should be investigated in the future.

Helices with core Lys residues maintained a transmembrane state down to pH 4, and thus do not seem to form the charged state even at 6−8 pH units below their pK_a values in solution. This raises the question of why the core Lys do not protonate at low pH. This can be explained by assuming the end(s) of the peptides become(s) somewhat buried in the bilayer when an ionizable residue in the core becomes charged and the peptide as a whole moves to the surface (Figure 5, bottom). If the ends become buried in the membrane, then in order to protonate a core Lys it might be necessary to simultaneously **deprotonate** one or more flanking Lys residues. This combination of protonation and deprotonation could be energetically unfavorable because low pH would be stabilizing the protonation of the flanking Lys residues (so that they resist burial within the bilayer) at the same time it increases the tendency of the core Lys residue to protonate. In contrast, high pH favors both of the changes that may be needed to form the S state, deprotonation of both the core Asp (driving movement toward the surface) and flanking Lys (so that they do not resist deeper insertion). This hypothesis may be testable by examining the behavior of pLeu helices in which the flanking residues are changed from Lys to polar residues.

It is important not to overgeneralize the (apparent) inability of buried ionizable residues to exist in a charged state. In proteins with multiple membrane-spanning segments, ionizable residues could potentially exist in a charged state if they face away from the lipid and toward other protein segments or an aqueous pore.

Comparison to the Behavior of Hydrophobic Helices Biosynthetically Incorporated into Natural Membranes. Several methods to evaluate the behavior of hydrophobic helices by natural biosynthesis have recently been developed (*24, 30, 31*). The behavior of pLeu-type helices (mostly in the context of a two-helix protein) in natural membranes has been investigated in a recent series of elegant studies by von Heijne and colleagues [e.g., (*8, 31*)]. The glycosylation mapping system they established involves identification of the residue at the membrane insertion boundary on one side of a hydrophobic helix based on its distance to the nearest residue accessible to glycosylation during biosynthesis. Using this system, they also found that interrupting a hydrophobic sequence by placing an ionizable residue (which they described as "charged" residues) near the center of the hydrophobic core did not prevent transmembrane insertion (*8*).

The glycosylation mapping system may have certain limitations relative to the artificial membrane system used in this report. First, it only probes helix structure at the time of glycosylation, when the sequence is likely to be interacting with the translocon proteins instead of, or in addition to, membrane lipids. Although some experiments show that the structure at the time of glycosylation often accurately reflects final topography (*31*), others suggest topography is flexible at this stage of protein folding and can be influenced by glycosylation (*32*). In addition, this method cannot be used to investigate the effect of certain key experimental parameters, such as the pH or the effect of lipid structure, upon helix topography.

On the other hand, the glycosylation mapping system has many advantages. For example, it allows a rapid scan of many sequences. Also, it can be used to look at hydrophobic sequences that are too long to efficiently synthesize by chemical methods. Furthermore, precisely because it involves topography during synthesis it yields information about the stability and nature of the transmembrane state during its formation.

---

[3] It is unlikely that the highly red-shifted fluorescence of pLeu(D11) and the lack of concentration dependence at high pH reflect a stronger tendency to oligomerize relative to the other peptides rather than an Asp ionization event which changes peptide depth. The former explanation would not account for the change in Trp depth observed at high pH.

[4] It should be remembered that for a linked ionization equilibrium, in which both a membrane buried and a surface species exist, the apparent pK_a is determined by a combination of equilibria for the buried and surface species (*34*).

[5] There are two reasons that quenching may report a slightly deeper Trp depth than predicted from this model. One is that the depth measured by fluorescence quenching may give only a lower estimate to the actual Trp depth. The reason for this is that the quenching analysis assumes that the lateral approach of a quenching molecule is not a function of quencher depth. This is not the case when a peptide orients parallel to the bilayer surface. A peptide so oriented, and located close to the bilayer surface, would tend to block the approach of a shallow quenching group to a greater degree than a deep quenching group, exaggerating quenching by the deep quencher and thus exaggerating apparent depth (*33*). The second explanation is that even at high pH there could some fraction of a transmembrane orientation present.

There are also differences between the glycosylation mapping and artificial membrane approach in terms of the information they yield. The former method identifies the residue at one membrane boundary, whereas the method in this report examines the position of the center of the hydrophobic sequence. In addition, effects due to helix oligomerization are more likely to be encountered in the artificial membrane system. Oligomerization can be a serious complication in some experiments, but it is also a parameter of interest. It should be noted other new natural membrane methods promise to yield much information about helix oligomerization (*24*, *30*). Overall, the artificial membrane and natural membrane biosynthesis approaches should be seen as complementary, and together promise to provide a much more detailed picture of the interactions important for establishing membrane protein folding and orientation than has been available up to the present.

REFERENCES

1. Henderson, R., Baldwin, J. M., Ceska, T. A., Zemlin, F., Beckmann, E., and Downing K. H. (1990) *J. Mol. Biol*. *213*, 899−929.
2. Landolt-Marticorena, C., Williams, K. A., Deber, C. M., and Reithmeier, R. A. F. (1993) *J. Mol. Biol. 229*, 602−608.
3. MacKenzie, K. R., Prestegard, J. H., and Engelman, D. R. (1997) *Science 276*, 131−133.
4. Lemmon, M. A., Flanagan, J. M., Treutlein, H. R., Zhang, J., and Engelman, D. M. (1992) *Biochemistry 31*, 12719−12725.
5. Smith, S. O., Smith, C. S., and Bormann, B. J. (1996) *Nat. Struct. Biol. 3*, 252−258.
6. Cosson, P., Lankford, S. P., Bonifacio, J. S., and Klausner, R. D. (1991) *Nature 351*, 414−416.
7. Ren, J., Lew, S., Wang, Z., and London, E. (1997) *Biochemistry 36*, 10213−10220.
8. Monne, M., Nilsson, I., Johansson, M., Elmhed, N., and von Heijne, G. (1998) *J. Mol. Biol*. *284*, 1177−1183.
9. Bolen, E. J., and Holloway, P. W. (1990) *Biochemistry 29*, 9638−9643.
10. Huschilt, J. C., Millman, B. M., and Davis, J. H. (1989) *Biochim. Biophys. Acta 979*, 139−141.
11. Webb, R. J., East, J. M., Sharma, R. P., and Lee, A. G. (1998) *Biochemistry 37*, 673−679.
12. Ren, J., Lew, S., Wang, J., and London, E. (1999) *Biochemistry 38*, 5905−5912.
13. Liu, L.-P., and Deber, C. M. (1997) *Biochemistry 36*, 5476−5482.
14. Lew, S., and London, E. (1997) *Anal. Biochem. 251*, 113−116.
15. Abrams, F. S., and London, E. (1993) *Biochemistry 32*, 10826−10831.
16. Jones, J. D., and Gierasch LM. (1994) *Biophys. J. 67*, 1534−1545.
17. Chattopadhyay, A., and London, E. (1987) *Biochemistry 26*, 39−45.
18. Abrams, F. S., and London, E. (1992) *Biochemistry 31*, 5312−5322.
19. Asuncion-Punzalan, E., and London, E. (1995) *Biochemistry 34*, 11460−11466.
20. Kachel, K., Asuncion-Punzalan, E., and London, E. (1995) *Biochemistry 34*, 15475−15479.
21. Kachel, K., Asuncion-Punzalan, E., and London, E. (1998) *Biochim. Biophys. Acta 1374*, 63−76.
22. Kaiser, R. D., and London, E. (1998) *Biochemistry 37*, 8180−8190.
23. Caffrey, M., and Feigenson, G. W. (1981) *Biochemistry 20*, 1949−1961.
24. Gurezka, R., Laage, R., Brosig, B., and Langosch, D. (1999) *J. Biol. Chem. 274*, 9265−9270.
25. Killian, J. A. (1998) *Biochim. Biophys. Acta 1376*, 401−416.
26. Chung, L. A., and Thompson, T. E. (1996) *Biochemistry 35*, 11343−11354.
27. Zhang, Y.-P., Lewis, N. A. H., Henry, G. D., Sykes, B. D., Hodges, R. S., and McElhaney, R. N. (1995) *Biochemistry 34*, 2348−2361.
28. Abrams, F. S., Chattopadhyay, A., and London, E. (1992) *Biochemistry 31*, 5322−5327.
29. Hristova, K., Wimley, W. C., Mishra, V. K., Anantharamiah, G. M., Segrest, J. P., and White, S. H. (1999*) J. Mol. Biol. 290*, 99−117.
30. Russ, W. P., and Engelman, D. M. (1999) *Proc. Natl. Acad. Sci. U.S.A. 96*, 863−868.
31. Nilsson, I., Saaf, A., Whitley, P., Gafvelin, G., Waller, C., and von Heijne, G. (1998) *J. Mol. Biol*. *284*, 1165−1175.
32. Goder, V., Bieri, C., and Speiss, M. (1999) *J. Cell Biol. 147*, 257−265.
33. Malenbaum, S. E., Collier, R. J., and London, E. (1998) *Biochemistry 37*, 17915−17922.
34. Hunt, J. F., Rath, P., Rothschild, K. J., and Engelman, D. M. (1997) *Biochemistry 36*, 15177−15192.
35. de Planque, M. R. R., Kruijtzer, J. A. W., Liskamp, R. M. J., Marsh, D., Greathouse, D. V., Koeppe, R. E., II, de Kruijff, B., and Killian, J. A. (1999) *J. Biol. Chem. 274*, 20839−20846.

BI000694O